Am J Cancer Res 2026;16(1):88-104
www.ajcr.us /ISSN:2156-6976/ajcr0169597

Original Article

Diagnostic value of mitochondria-related genes in intervertebral disc degeneration associated with spinal metastasis: a Mendelian randomization study

Lei Liu[1,2*], Yuanhao Liang[3*], Bin Shi[4], Gongchang Yu[4], Shengxin Peng[5], Yixiang Zhang[3], Wenshan Xiao[6], Rui Xu[1]

[1]Academy of Medical Engineering and Translational Medicine, Tianjin University, Tianjin, China; [2]Department of Painology, The First Affiliated Hospital of Shandong First Medical University (Shandong Provincial Qianfoshan Hospital), Jinan, Shandong, China; [3]Weifang Medical University, Weifang, Shandong, China; [4]Neck-Shoulder and Lumbocrural Pain Hospital of Shandong First Medical University, Shandong First Medical University and Shandong Academy of Medical Sciences, Jinan, Shandong, China; [5]School of Rehabilitation Medicine of Binzhou Medical University, Yantai, Shandong, China; [6]Shandong First Medical University, Jinan, Shandong, China. [*]Co-first authors.

Received October 27, 2025; Accepted January 4, 2026; Epub January 15, 2026; Published January 30, 2026

Abstract: To identify mitochondria related genes involved in intervertebral disc degeneration (IDD) and to investigate the potential molecular mechanism. The GSE124272 and GSE56081 datasets were used in this study. First, intersecting genes were screened by overlapping key module genes obtained from weighted gene co-expression network analysis (WGCNA) and differentially expressed genes (DEGs). Functional enrichment analyses were performed to explore the functions of intersecting genes. Subsequently, candidate IDD-associated genes were screened using Mendelian randomization (MR) based on the intersecting genes. Thereafter, machine learning algorithm was applied to identify biomarkers, and their diagnostic performance was assessed using receiver operating characteristic (ROC) curves. Single-gene gene set enrichment analysis (GSEA) was utilized to investigate the molecular mechanisms of the identified biomarkers. Meanwhile, correlations between the biomarkers and immune cell infiltration were investigated. In addition, the transcription factor (TF)-mRNA and competing endogenous RNA (ceRNA) networks were constructed. Finally, the mRNA-drug interaction network was established. A total of 827 intersecting genes were screened, and 31 differentially expressed mitochondria-related genes were obtained. Functional enrichment results revealed that these genes were primarily involved in the positive regulation of cytokine production and the cell cycle. Four candidate genes were obtained by MR analysis based on intersecting genes. Finally, two biomarkers (PTGS1 and PPBP) were screened, both of which demonstrated decent diagnostic performance. Single-gene GSEA enrichment results indicated that these two biomarkers were mainly enriched in the ribosome and neuroactive ligand receptor interaction. Correlation analysis showed strongest positive correlation between PTGS1 and mast cells, and the highest negative association between PPBP and activated CD4 T cells. The mRNA-TF regulatory network included 2 mRNAs, 12 TFs, and 15 pairs of regulatory interactions. Furthermore, the ceRNA regulatory network included 2 biomarkers, 45 miRNAs, and 67 long non-coding RNA (lncRNAs). Finally, a total of 70 potential drugs targeting these biomarkers were predicted. In conclusion, PTGS1 and PPBP were identified as key mitochondria-related genes associated with IDD, providing novel insights into the diagnosis and treatment of IDD.

Keyword: Intervertebral disc degeneration, mitochondria-related genes, signature genes, Mendelian randomization, spinal metastases

Introduction

The spine is the most common site of bone metastases and the incidence of spinal metastases is on a rise [1]. Up to 70% of cancer patients develop spinal metastases, among whom approximately 10% subsequently experience metastatic cord compression [2]. Spinal metastases predominantly originate from a defined spectrum of primary tumors, including breast, lung, prostate, and renal cancers, while thyroid cancer, melanoma, myeloma, lympho-

https://doi.org/10.62347/MIVG6273

ma, and colorectal carcinoma are less common [3]. Over the last decades, survival in patients with spinal metastases has significantly increased due to the advances in molecular characterization of tumors, surgical techniques, chemotherapy, radiotherapy and hormonal therapies [4]. With the improvement in long-term survival rates for patients with spinal metastases, the survivor population continues to expand. This makes it increasingly important to gain a deeper understanding of the long-term late effects caused by spinal metastases and their treatments. Current management strategies include chemotherapy, radiotherapy, surgical excision, or a combination of these approaches. Previous studies have shown that while spinal radiotherapy is clinically feasible, immature organ systems are prone to radiation damage. Therefore, radiotherapy in generally not recommended in young patients.

Intervertebral disc degeneration (IDD) has been increasingly observed in long-term survivors of spinal metastases, especially among patients undergoing spinal radiotherapy [5]. Studies have reported a higher prevalence of lumbar IDD in patients with spinal metastases [6]. Resnick et al. reported that intervertebral disc abnormalities was associated with spinal metastasis from prostatic carcinoma, identifying intervertebral disc degeneration, cartilaginous nodes, and disc invasion by tumor as potential pathological processes [7]. Similarly, Jónsson et al. found that endplate defects and depressions in spine specimens affected by breast cancer metastases were associated with compensatory expansion of the intervertebral discs, which contributes to IDD [8]. Nucleus pulposus (NP) cells are essential for the intervertebral disc function and extracellular matrix metabolism, which undergo the earliest degenerative changes during the process of IDD [9]. Thus, a comprehensive understanding of molecular mechanisms underlying NP cell loss may offer a new insights into relieving IDD caused by spinal metastases.

Mitochondria are double-membrane-bound organelles primarily responsible for adenosine triphosphate production. They can activate multiple enzymes involved in oxidative metabolic pathways. Mitochondrial dysfunction has been associated with cell damage and various age-related diseases [10]. Some studies have revealed that mitochondria-induced cell death is a critical mechanism contributing to IDD [11]. Moreover, mitochondrial damage has been associated with NP cell dysfunction, metabolic imbalance between anabolic and catabolic processes, and inflammatory responses [12]. Disruption of mitochondrial dynamics has also been positively associated with oxidative stress in the process of IDD [13]. To date, most studies on mitochondria-related genes have primarily focused on their regulation of mitochondrial function. However, emerging evidence suggests that mitochondrial-related genes are also closely associated with cell function and immune regulation [14]. Given that the intervertebral disc (IVD) is immune-privileged under physiological conditions, elucidating the roles of mitochondrial-related genes in the process of IDD has become a hotspot of research.

In this study, IDD-related datasets were integrated with Mendelian randomization (MR) analysis to identify differentially expressed mitochondria-related genes associated with IDD. The biological pathways and molecular regulatory networks involving these genes were explored, and the potential pharmaceuticals were further investigated. The findings of this study would offer new theoretical insights and evidence for the treatment of IDD.

Materials and methods

Source of data

The GSE124272 and GSE56081 datasets were sourced from the Gene Expression Omnibus (GEO) database (https://www.ncbi.nlm.nih.gov/geo/). The GSE124272 dataset (GPL570) included whole-blood microarray data from 8 control samples and 8 IDD samples derived from patients with spinal metastases. The GSE56081 dataset (GPL10295) included the microarray data of human nucleus pulposus tissue from 5 patients with IDD secondary to spinal metastases and 5 control samples. A total of 1136 mitophagy-related genes (MRGs) were obtained from the MitoCarta 3.0 database (https://www.broadinstitute.org/mitocarta) [15]. The ukb-b-19807 dataset was sourced from the IEU OpenGWAS database (https://gwas.mrcieu.ac.uk/). The ukb-b-19807 dataset included the single nucleotide polymorphism (SNP) data from 463,010 IDD samples (9,851,867 SNPs).

Identification of differentially expressed genes (DEGs)

DEGs between the IDD and control groups were identified in the GSE124272 dataset using the *limma* package (version 3.52.4) [16], with a *P* value < 0.05 and $|\log_2 FC| \geq 0.5$. Volcano plots and heatmaps were drawn using the *ggplot2* package (version 3.3.6) [17] and the *heatmap3* package (version 1.1.9), respectively, illustrating the variance of DEGs.

Screening of key module genes using weighted gene co-expression network analysis (WGCNA)

The MRG score of each sample was obtained using the *GSVA* package (version 1.44.5) [18], with MRGs serving as the reference gene set. WGCNA (version 1.71) was then performed to [19] screen genes associated with the MRG score. Initially, sample clustering was performed to remove potential outliers, thereby ensuring the accuracy of the analysis. Then, the optimal soft-threshold (β) was selected to construct a scale-free co-expression network. Next, the clustering dendrogram was acquired by calculating the adjacency and similarity. Gene modules were identified using the dynamic tree-cutting algorithm. The correlations between each module and the MRG score were then evaluated, and the modules with the strongest correlation was defined as the key module. Lastly, genes in the key module were targeted as key module genes for subsequent analyses.

Acquisition and functional annotation of intersection genes

The *UpSetR* package (version 1.4.0) [20] was utilized to identify overlapping DEGs and key module genes, designating as intersection genes. Gene Ontology (GO) and Kyoto Encyclopedia of Genes and Genomes (KEGG) enrichment analyses of intersection genes was performed using the *clusterProfiler* package (version 4.4.4) (*P* value < 0.05) [21].

Mendelian Randomization (MR) analysis

The intersection genes were used as exposure variables and IDD as the outcome variable for MR analysis. MR analysis is based on three assumptions: ① there is a strong correlation between instrumental variables and exposure; ② instrumental variables are independent of confounding factors affecting both the exposure and the outcome; and ③ the instrumental variables influence the outcome only through the exposure, rather than other biological pathways.

First, the reading and filtering of exposure factors was carried out using the *mv_harmonise_data* function of the *TwoSampleMR* package (version 0.5.6) [22]. The *mv_lasso_feature_selection* function was utilized to eliminate collinearity among instrumental variables, and then the *mv_multiple* function along with five algorithms MR-Egger [23], Weighted median [24], Simple mode, Weighted mode [25] and inverse variance weighted (IVW) regression [26] were employed for MR analysis. The IVW method was considered the primary approach for causal inference. Then, odds ratios (ORs) were calculated to estimate effect sizes, with OR > 1 indicating risk factor and OR < 1 indicating protective factor. The results were visualized using scatter plots and funnel plots. The robustness of the MR results was assessed using sensitivity analyses, including heterogeneity test, horizontal pleiotropy test, and the Leave-One-Out (LOO) method. The final screened significant exposures were defined as candidate genes for subsequent analyses.

Machine learning and subcellular localization analysis

Candidate genes were further screened to identify biomarkers using support vector machine-recursive feature elimination (SVM-RFE) algorithm implemented in the e1071 package (version 1.7-11). Then, the predictive accuracy of the identified biomarkers was evaluated using receiver operator characteristic (ROC) curves based on the GSE124272 and GSE56081 datasets. Meanwhile, differences in the expression of biomarkers between IDD and control groups were compared in both datasets. In addition, a gene-gene interaction (GGI) network of the biomarkers was constructed using GeneMANIA platform (http://genemania.org), with the top 20 genes displayed. Finally, sub-cellular distribution of the identified biomarkers was determined using the Genecards databased, with a confidence score threshold set at 5.

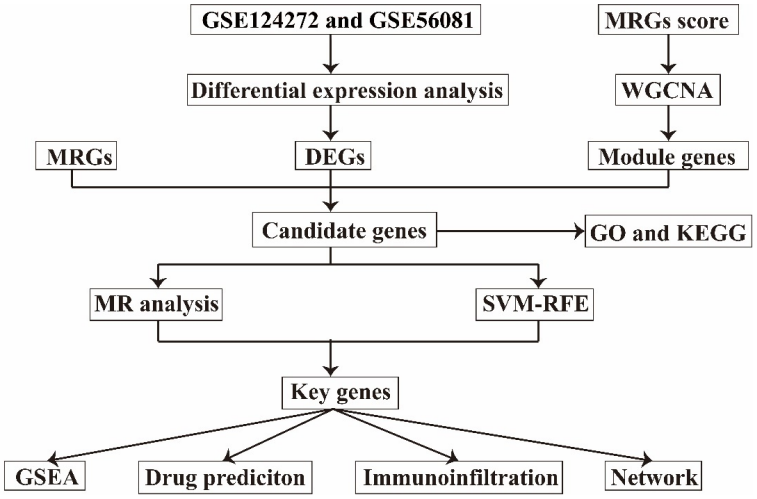

Figure 1. Workflow of this study. This study integrated differential expression analysis, WGCNA, and machine learning to identify mitochondria-related candidate genes associated with IDD. Key genes were validated through MR analysis and SVM-RFE, followed by functional enrichment analysis, regulatory network construction, immune infiltration analysis, and prediction of potential treatment drugs. Notes: WGCNA, weighted gene co-expression network analysis; MR, Mendelian randomization; SVM-RFE, support vector machine-recursive feature elimination; IDD, intervertebral disc degeneration.

Single-gene gene set enrichment analysis (GSEA)

Single-gene GSEA was performed to explore the potential regulatory pathways and biological functions associated with each biomarker. Pathways with adjusted *P* value < 0.05 were considered statistically significant. The top 5 significantly enriched KEGG pathways were visualized separately.

Immune-infiltration analysis

The proportion of 28 immune cell subtypes in each sample were computed using the single-sample GSEA algorithm in the GSVA package (version 1.44.5) [27]. Differences in immune cell infiltration between the IDD and control groups were subsequently compared, and the results were visualized using box plots. Meanwhile, the correlation analysis was performed between immune cells and biomarkers using Spearman method.

Construction of the mRNA-transcription factor regulatory network

Transcription factors (TFs) targeting the identified biomarkers were predicted using the miRNet (https://www.mirnet.ca/) based on the JASPAR database (degree ≥ 1). Then, the mRNA-TF regulatory network was constructed and visualized using Cytoscape software (version 3.9.1) [28].

Construction of the competing endogenous RNA (ceRNA) regulatory network

miRNAs targeting the identified biomarkers were predicted using miRNet (https://www.mirnet.ca/) based on the JASPAR database (degree ≥ 1). Interactions between lncRNAs and miRNAs were obtained from the Starbase database (clipExpNum ≥ 20). Finally, the lncRNA-miRNA-mRNA network was constructed using Cytoscape software (version 3.9.1).

Construction of biomarker-drug interaction network

Potential drugs interacting with the identified biomarkers were retrieved from the DrugBank database (https://go.drugbank.com/). A biomarker-drug interaction network was constructed based on the predicted results (screening of approved drugs). Then, the network was visualized using Cytoscape software (version 3.9.1).

Statistical analysis

All bioinformatics analyses were conducted using R language software (version 4.1.2). SPSS version 22.0 was used for statistical analyses. Spearman's correlation method was used for correlation analysis. A two-sided *P* value < 0.05 was considered statistically significant.

Results

Identification of DEGs and key module genes

The overall analytical design is illustrated in **Figure 1**. A total of 1493 DEGs were identified between the IDD and control group from the GSE124272 dataset, among which 765 were

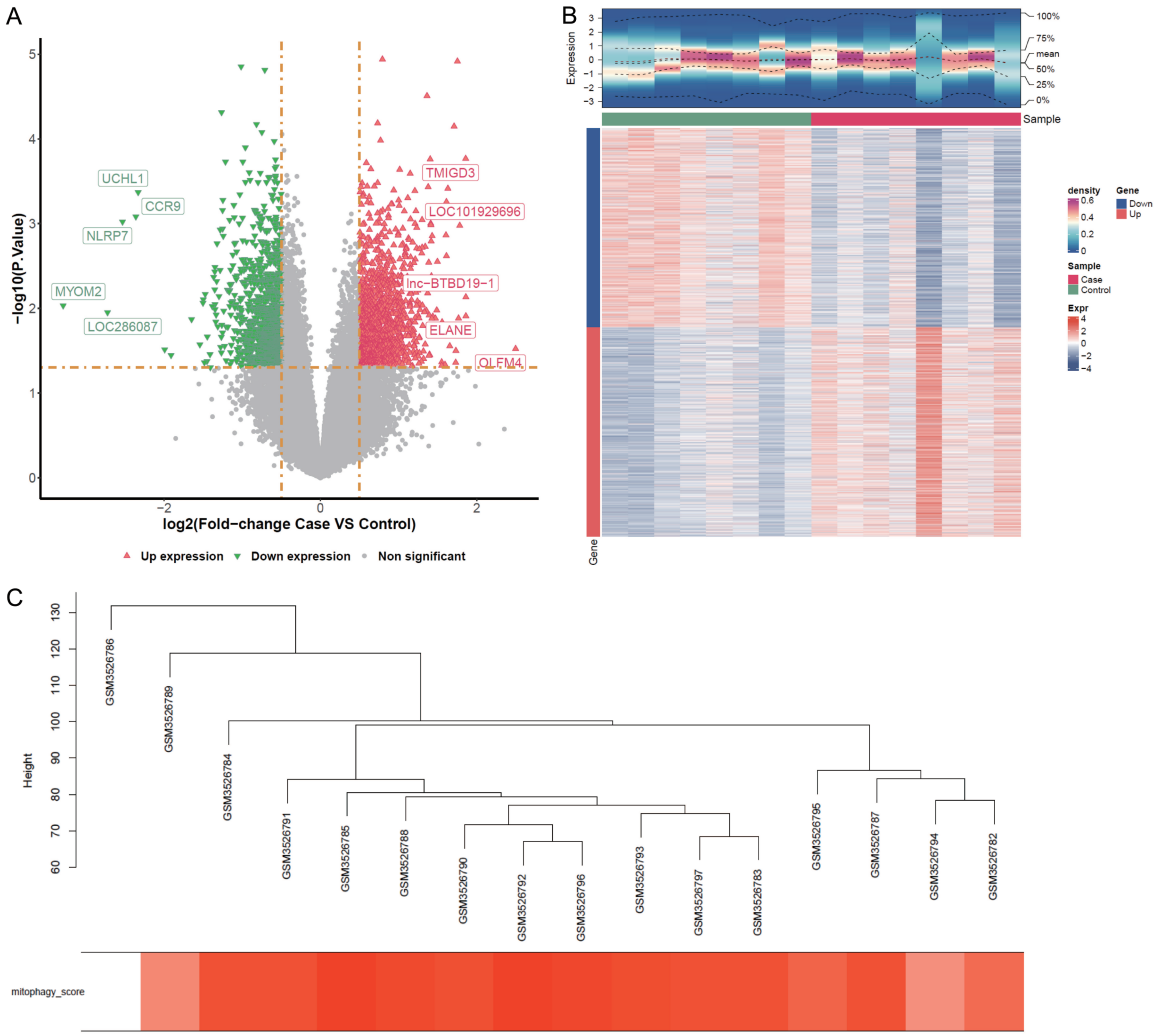

Figure 2. Identification of DEGs. A: Volcano plot showing DEGs between the IDD and control groups; B: Heatmap of DEGs; C: Venn diagram illustrating the DE-MRGs by overlapping MRGs and DEGs. Notes: DEG, differentially expressed gene; IDD, intervertebral disc degeneration; DE-MRGs, differentially expressed mitochondria-related genes; MRGs, mitochondria-related genes.

up-regulated and 728 were down-regulated (**Figure 2A** and **2B**). WGCNA analysis was performed on the GSE124272 dataset to identify genes related to MRG scores. Sample clustering results demonstrated the absence of outlier samples (**Figure 2C**). When the soft threshold was set to 10, the resulting network best approximated a scale-free topology (R^2 = 0.85), with the average connectivity close to zero. Then, a total of 17 modules were obtained after merging similar modules by setting MEDissThres to 0.3 (**Figure 3A** and **3B**). Of these, MEblue (r = 0.82, P = 9e-05) exhibited the strongest correlation with the MRG score (**Figure 3C**). Hence, this module was defined as key module, containing 8941 genes that recognized as key module genes for subsequent analyses.

Functional enrichment analysis of intersection genes

A total of 827 intersection genes, including NLRP7, CCR9, UCHL1, GLDC, P3H2, TNFRSF17, were obtained (**Figure 4A**). Among these, 31 DE-MRGs were identified (**Figure 4B**). Enrichment analysis indicated that these genes were involved in 546 GO terms, comprising 51 cellular component (CC), 53 molecular function (MF), and 442 biological process (BP) categories, and 10 KEGG pathways. GO enrichment analysis indicated that these genes were pri-

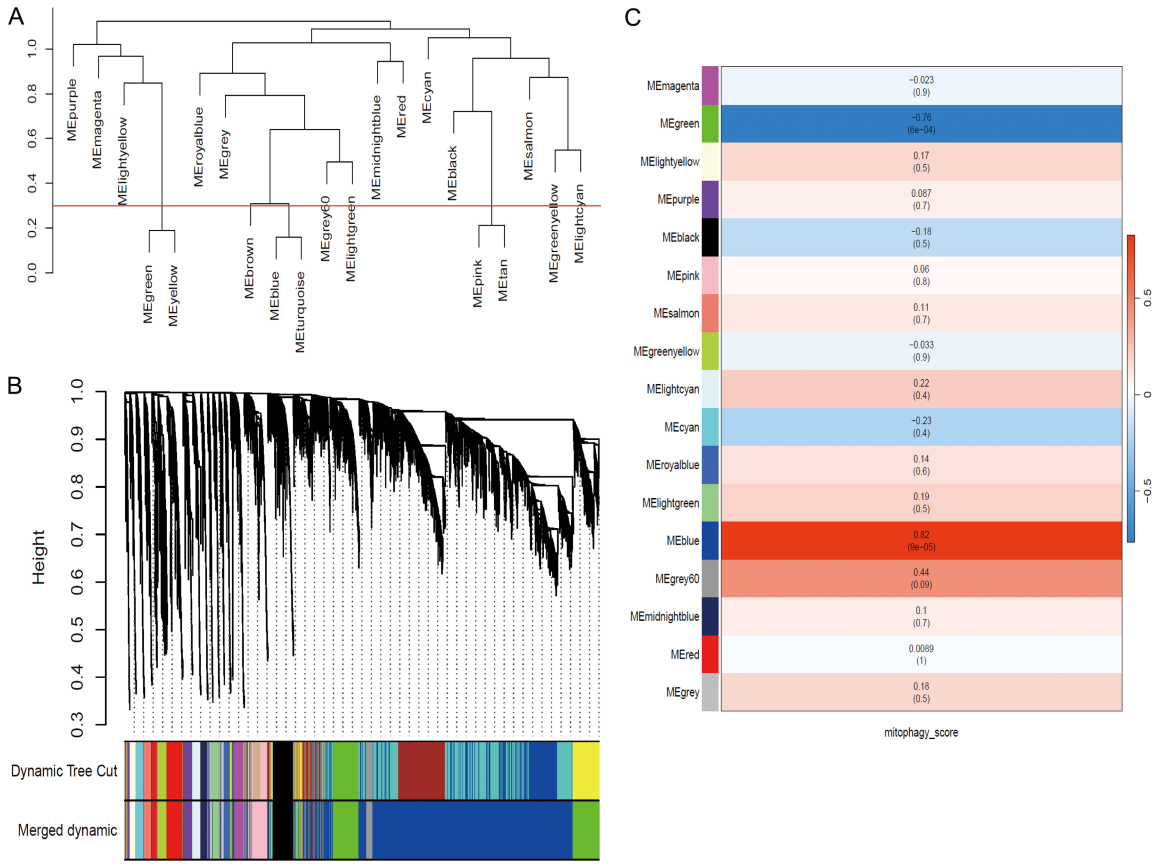

Figure 3. Identification of key module genes. A: Clustering dendrogram of module eigengenes; B: Gene dendrogram with corresponding module colors; C: Correlations between module eigengenes and MRG scores. Note: MRGs, mitochondria-related genes.

marily associated with positive regulation of cytokine productions and the Fc receptor signaling pathway (**Figure 4C**). KEGG analysis demonstrated significant enrichment in pathways including the cell cycle, protein processing in the endoplasmic reticulum (**Figure 4D**).

Screening of candidate genes for IDD and sensitivity analysis

A total of 4 candidate genes were acquired through MR analysis, including PTGS1, SELP, PPBP, and PRRG4. The IVW method revealed causal relationship between IDD and PTGS1 (P = 0.0020; ORs = 1.00016), SELP (P = 0.0024; ORs = 1.00015), PPBP (P = 0.0343; ORs = 1.00011), and PRRG4 (P = 0.0386; ORs = 1.00045), indicating that these genes were all risk factors for IDD. Scatter plots generated using five algorithms demonstrated consistent directions of effect, with a small intercept and a positive slope for IVW. Funnel plots showed symmetrical distributions of instrumental variables, consistent with random allocation of alleles according to Mendel's second law.

Heterogeneity analysis revealed no significant heterogeneity among instrumental variables, and the Q values for PTGS1, SELP, PPBP, and PRRG4 were 0.1551, 0.1113, 0.6245 and 1.6059, respectively (**Table 1**). The results of the horizontal pleiotropy test indicated that there was no horizontal multi-effect (PTGS1: P = 0.8071, SELP: P = 0.9108, PPBP: P = 0.9113, PRRG4: P = 0.9461) (**Table 2**). In addition, the LOO analysis showed that no single instrumental variable disproportionately influenced the IVW estimates, indicating robust and reliable results (**Figure 5**). In conclusion, the above results suggested that PTGS1, SELP, PPBP, and PRRG4 were candidate genes associated with IDD.

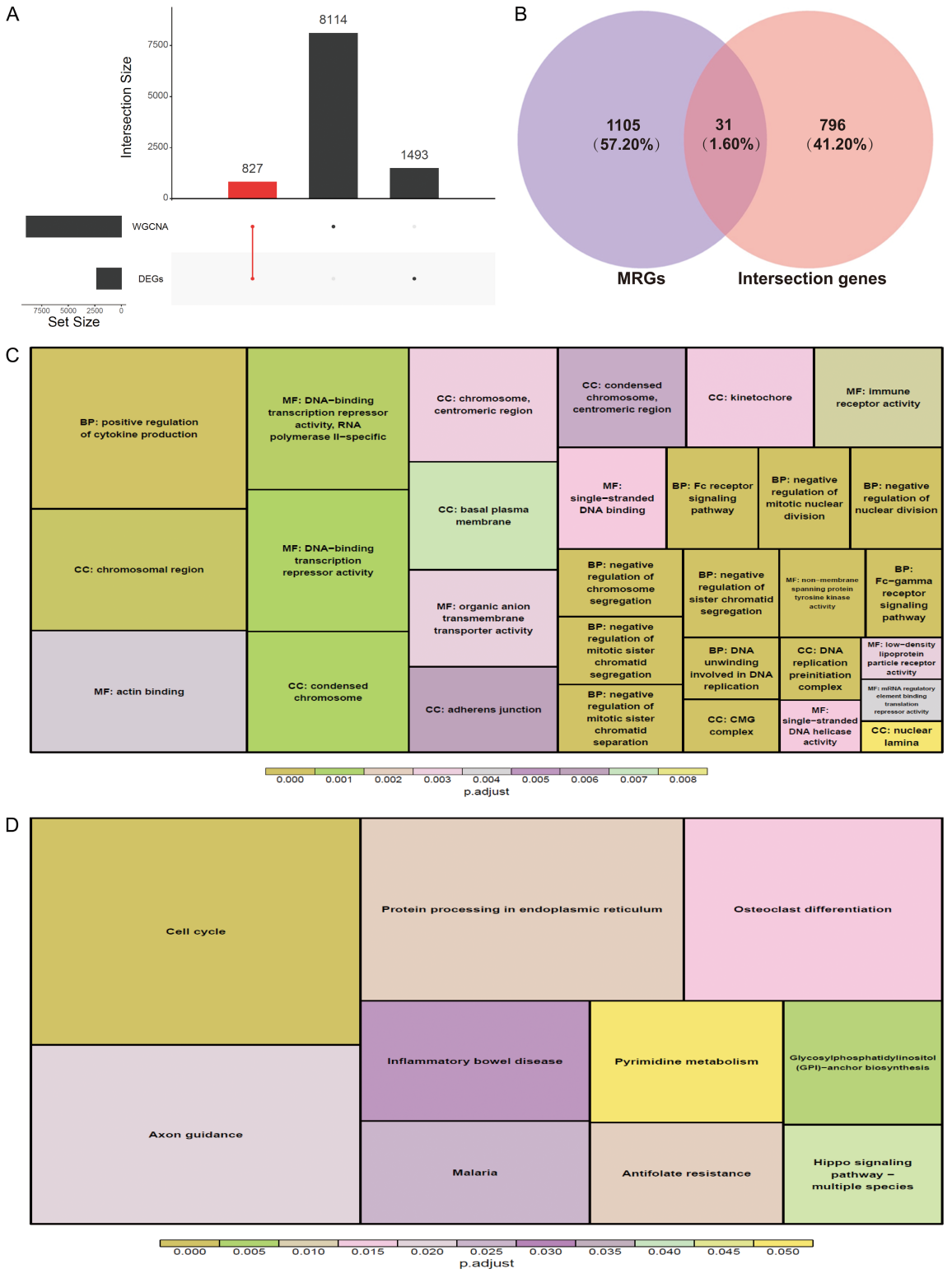

Figure 4. Functional enrichment of intersection genes. A: Identification of 827 intersection genes obtained by overlapping WGCNA-derived key module genes with DEGs; B: Venn diagram illustrating DE-MRGs identified by overlapping MRGs with intersection genes; C: GO enrichment analysis of intersection genes; D: KEGG pathway enrichment analysis of intersection genes. Notes: WGCNA, weighted gene co-expression network analysis; DE-MRGs, differentially expressed mitochondria-related genes; MRGs, mitochondria-related genes; DEG, differentially expressed gene; GO, Gene Ontology; KEGG, Kyoto Encyclopedia of Genes and Genomes.

Table 1. Heterogeneity test for PTGS1, SELP, PPBP and PRRG4

	Outcome	Exposure	Method	Q	Q_df	Q_pval
PTGS1	Diagnoses-main ICD10: M51.3 Other specified intervertebral disk degeneration || id:ukb-b-19807	ENSG00000095303 || id:eqtl-a-ENSG00000095303	MR Egger	0.078	2	0.962
	Diagnoses - main ICD10: M51.3 Other specified intervertebral disk degeneration || id:ukb-b-19807	ENSG00000095303 || id:eqtl-a-ENSG00000095303	Inverse variance weighted	0.156	3	0.984
SELP	Diagnoses - main ICD10: M51.3 Other specified intervertebral disk degeneration || id:ukb-b-19807	ENSG00000174175 || id:eqtl-a-ENSG00000174175	MR Egger	0.091	1	0.762
	Diagnoses - main ICD10: M51.3 Other specified intervertebral disk degeneration || id:ukb-b-19807	ENSG00000174175 || id:eqtl-a-ENSG00000174175	Inverse variance weighted	0.111	2	0.946
PPBP	Diagnoses - main ICD10: M51.3 Other specified intervertebral disk degeneration || id:ukb-b-19807	ENSG00000163736 || id:eqtl-a-ENSG00000163736	MR Egger	0.610	4	0.962
	Diagnoses - main ICD10: M51.3 Other specified intervertebral disk degeneration || id:ukb-b-19807	ENSG00000163736 || id:eqtl-a-ENSG00000163736	Inverse variance weighted	0.6245	5	0.987
PRRG4	Diagnoses - main ICD10: M51.3 Other specified intervertebral disk degeneration || id:ukb-b-19807	ENSG00000135378 || id:eqtl-a-ENSG00000135378	MR Egger	1.594	1	0.207
	Diagnoses - main ICD10: M51.3 Other specified intervertebral disk degeneration || id:ukb-b-19807	ENSG00000135378 || id:eqtl-a-ENSG00000135378	Inverse variance weighted	1.606	2	0.448

Table 2. Horizontal pleiotropy test for PTGS1, SELP, PPBP and PRRG4

	Outcome	Exposure	Egger_intercept	SE	pval
PTGS1	Diagnoses - main ICD10: M51.3 Other specified intervertebral disk degeneration || id:ukb-b-19807	ENSG00000095303 || id:eqtl-a-ENSG00000095303	-2.20E-05	7.90E-05	0.807
SELP	Diagnoses - main ICD10: M51.3 Other specified intervertebral disk degeneration || id:ukb-b-19807	ENSG00000174175 || id:eqtl-a-ENSG00000174175	-1.47E-05	0.000104492	0.911
PPBP	Diagnoses - main ICD10: M51.3 Other specified intervertebral disk degeneration || id:ukb-b-19807	ENSG00000163736 || id:eqtl-a-ENSG00000163736	-6.63E-06	5.59E-05	0.911
PRRG4	Diagnoses - main ICD10: M51.3 Other specified intervertebral disk degeneration || id:ukb-b-19807	ENSG00000135378 || id:eqtl-a-ENSG00000135378	-1.08E-05	0.000126817	0.946

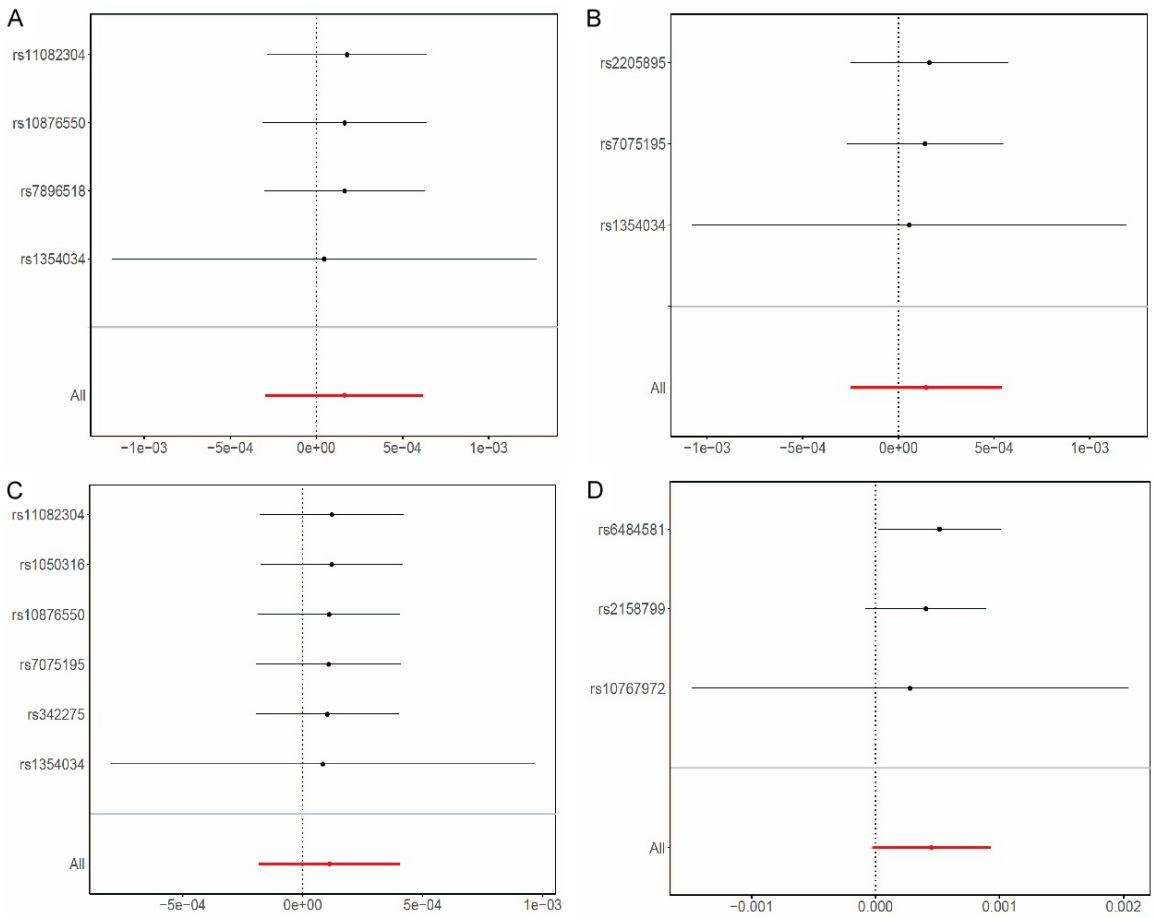

Figure 5. The sensitivity analysis of candidate genes using LOO analysis. A: PTGS1. B: SELP. C: PPBP. D: PRRG4. Note: LOO, leave-one-out.

Biomarker screening and performance evaluation

Through screening, a total of two biomarkers (PTGS1 and PPBP) were acquired using SVM-RFE algorithm (**Figure 6A**). Subcellular localization analysis revealed that PTGS1 and PPBP were predominantly distributed in endoplasmic reticulum and extracellular regions (**Figure 6B**). GGI network analysis indicated that the biomarkers interacted with genes such as PTGIS, TBXAS1, PTGDS, MPO, and PTGS2, and were mainly involved in biological functions including chemokine receptor binding and neutrophil migration (Supplementary Figure 1). ROC curve analysis demonstrated high diagnostic accuracy for both PTGS1 and PPBP, with area under the curve (AUC) values exceeding 0.79 in both the GSE124272 and GSE56081 datasets (**Figure 6C** and **6D**). These two biomarkers were all upregulated in IDD samples in both GSE124272 and GSE56081 datasets (**Figure 6E** and **6F**).

Single-gene GSEA analysis of biomarkers

Single-gene GSEA revealed that PTGS1 and PPBP were mainly enriched in KEGG pathways, including ribosome and neuroactive ligand-receptor interaction (**Figure 7A** and **7B**).

Immune-related analyses of biomarkers

A total of 7 immune cells, including activated CD4+ T cell, activated dendritic cell, and myeloid-derived suppressor cells (MDSCs), showed significant differences between the IDD and control groups (**Figure 8A**). Correlation analysis showed the strongest positive correlation between PTGS1 and the mast cell, and the strongest negative association between PPBP and the activated CD4 T cell (**Figure 8B**).

mRNA-TF and ceRNA regulatory networks of biomarkers

To further investigate the regulatory mechanisms of the identified biomarkers, mRNA-TF

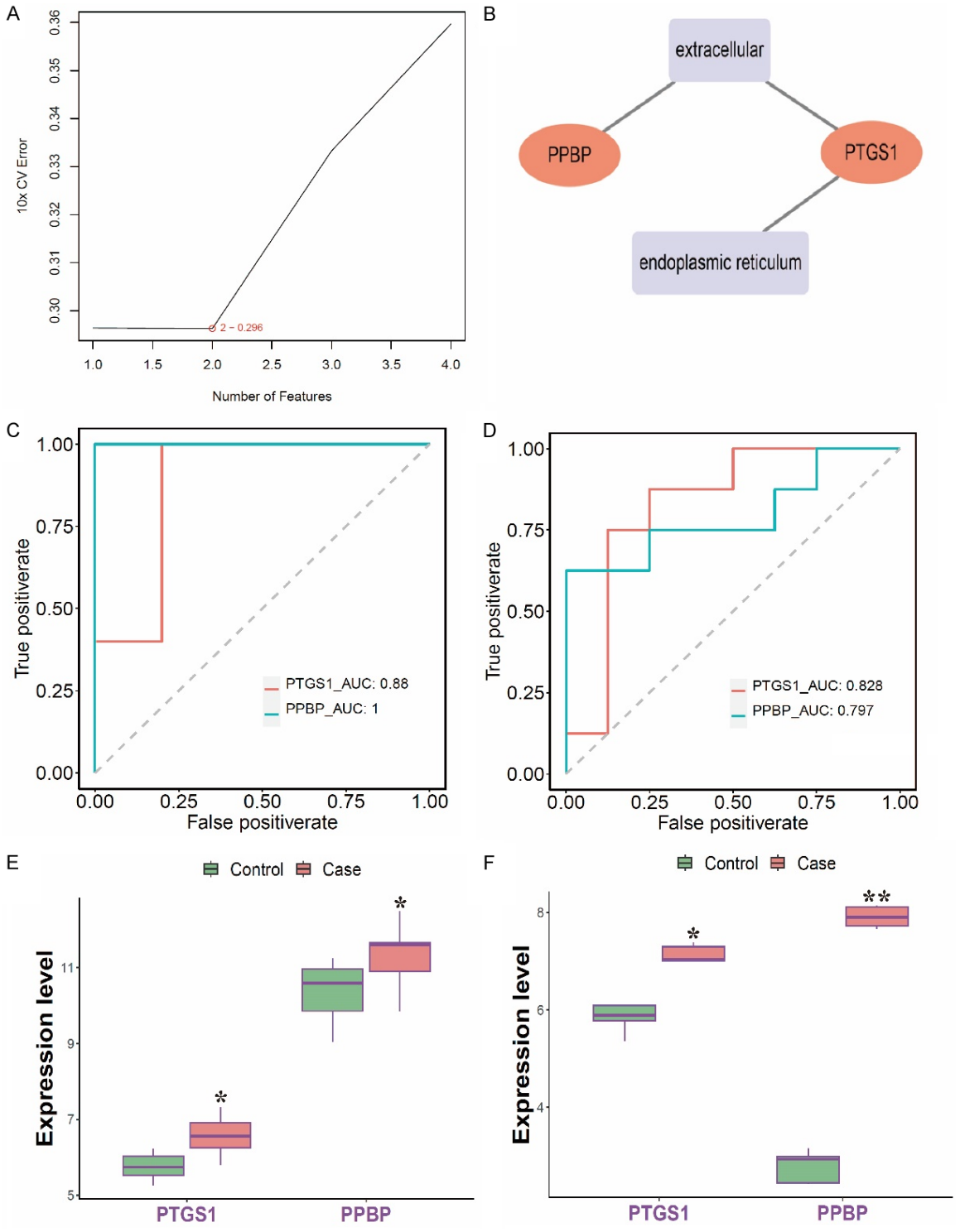

Figure 6. Biomarker screening and performance evaluation. (A) Top 2 genes with the minimum classification error for IDD selected based on SVM-RFE; (B) Subcellular localization of PTGS1 and PPBP; (C, D) ROC curve analysis showing the diagnostic performance of PTGS1 and PPBP in the GSE124272 dataset (C) and GSE56081 dataset (D); (E, F) Expression levels of PTGS1 and PPBP in the GSE124272 dataset (E) and GSE56081 dataset (F). Notes: SVM-RFE, support vector machine-recursive feature elimination; IDD, intervertebral disc degeneration.

and ceRNA regulatory networks were constructed. In total, 12 TFs corresponding to biomarkers were identified. Following this, an mRNA-TF regulatory network containing 14 nodes, in-

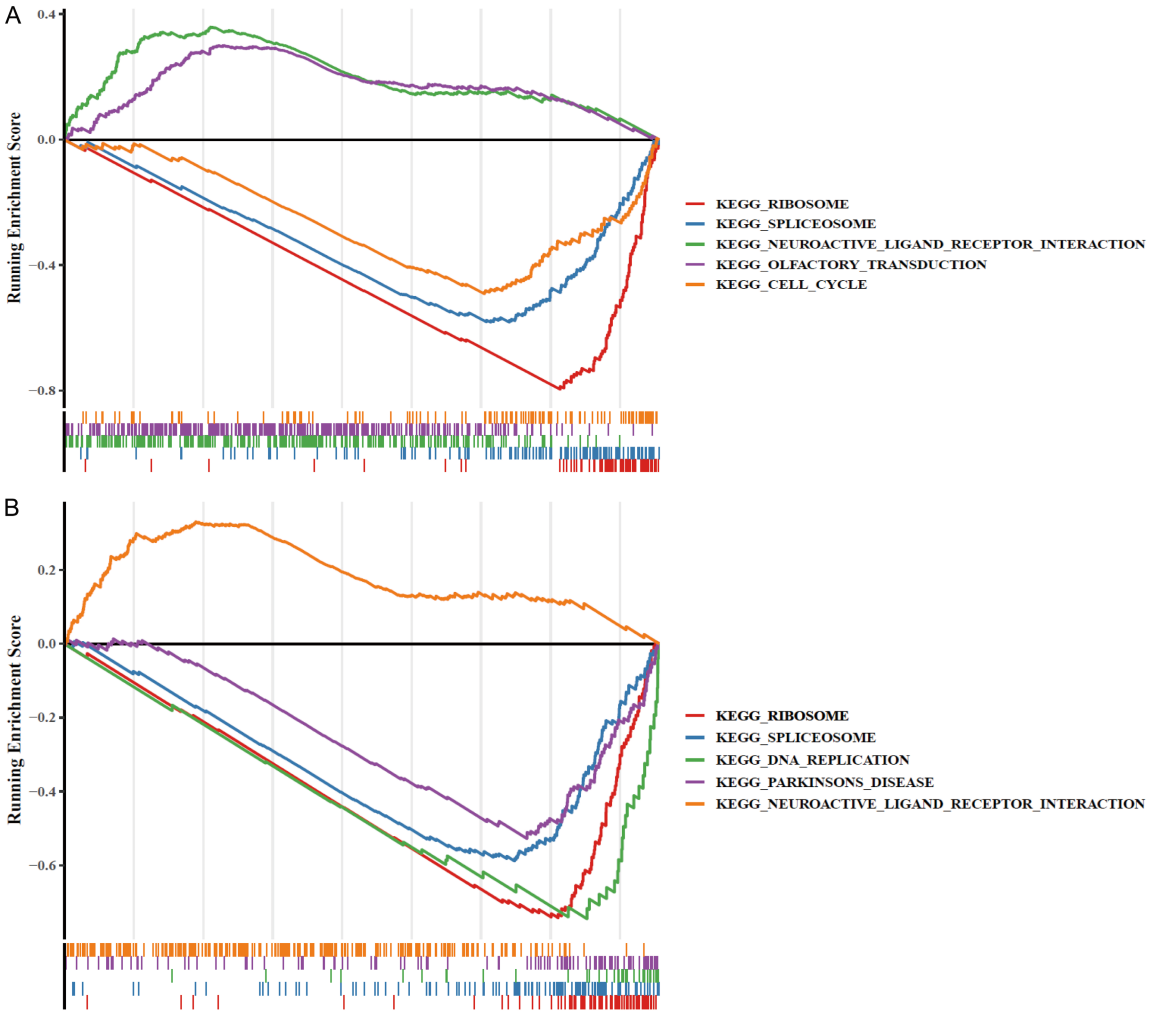

Figure 7. Single-gene GSEA analysis of biomarkers. A: PTGS1; B: PPBP. Note: GSEA, gene set enrichment analysis.

cluding 2 mRNAs (PTGS1 and PPBP) and 12 TFs (e.g., HOXA5, GATA2, RUNX2, and RUNX2) with 15 edges was established (Supplementary Figure 2A). Of these, PPBP was predicted to be regulated by a greater number of TFs. A lncRNA-miRNA-mRNA network was constructed by predicting 45 miRNAs targeting the biomarkers and integrating lncRNA-miRNA interaction data. This network contained 2 biomarkers (PTGS1 and PPBP), 45 miRNAs (e.g., hsa-miR-335-5p, hsa-miR-146b-3p, hsa-miR-4446-3p, and ahsa-miR-3173-5p), and 67 lncRNAs (e.g., AL513497.1, DANCR, HELLPAR, and miR497-HG) (Supplementary Figure 2B). Representative regulatory pairs included hsa-miR-130a-3p-PPBP and hsa-miR-101-3p-SNHG6.

Prediction of biomarker-related drugs

DrugBank database analysis identified 70 therapeutic drugs potentially targeting 2 biomarkers. Among these, 69 drugs (e.g., indomethacin, nabumetone, ketorolac, and tenoxicam) were predicted to interact with PTGS1 and one drug (copper) was predicted to target PPBP (**Figure 9**).

Discussion

The intervertebral disc (IVD) plays a crucial role in maintaining spinal flexibility and absorbing mechanical shocks. IDD secondary to spinal metastases can cause pain and constrain motion [29]. Although existing evidence has partially illustrated the pathogenic mechanisms underlying IDD caused by spinal metastases, studies specifically investigating mitochondrial dysfunction in this context remains limited. This study addressed this gap by integrating transcriptomic data and MR analysis to screen and verify key mitochondria-related genes involved in IDD. Furthermore, the biological pathways

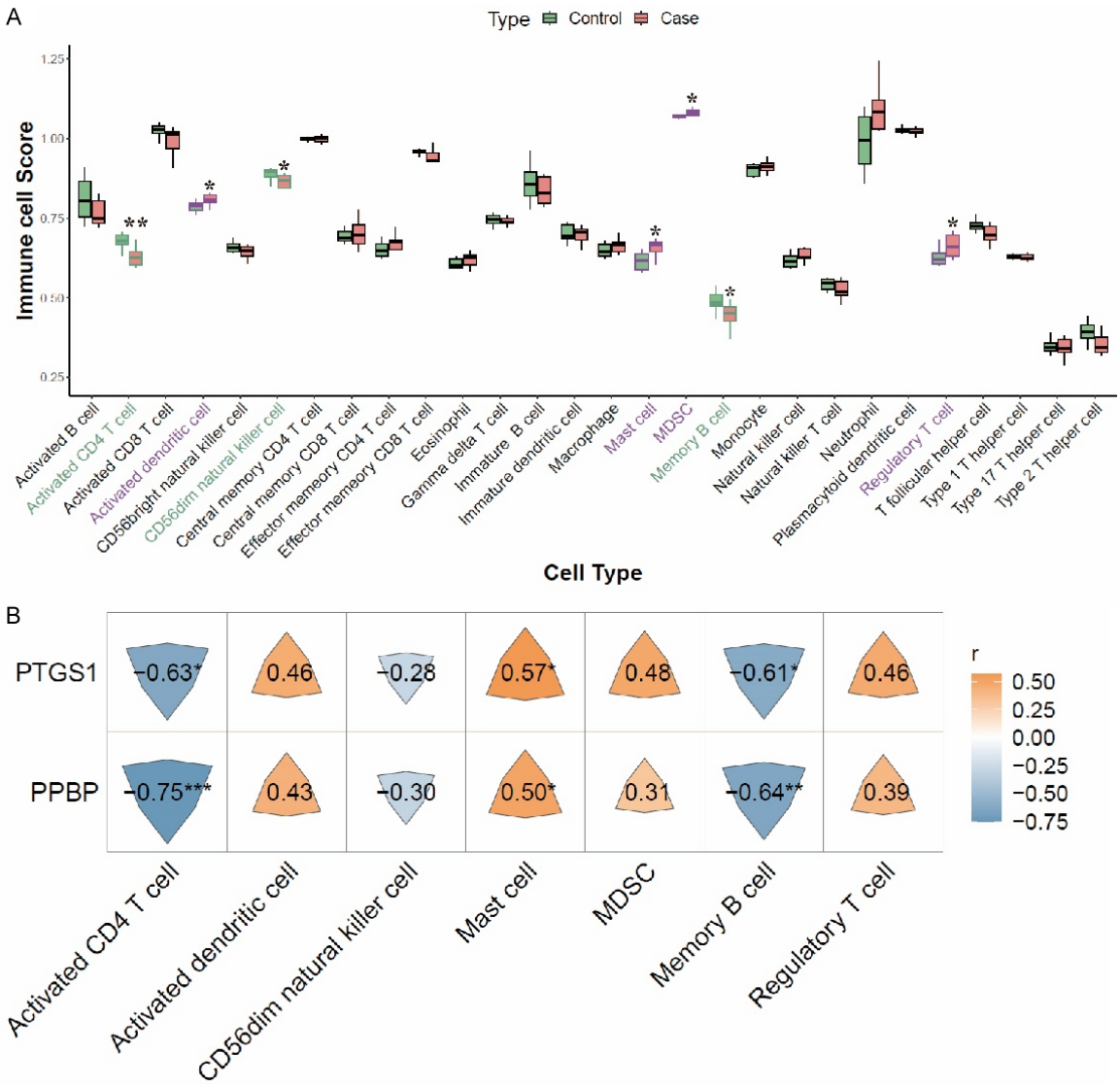

Figure 8. Immune-related analyses of biomarkers. A: Comparison of immune cell infiltration between IDD and control groups; B: Correlation analysis of PTGS1 and PPBP expression with immune cell infiltration.

and regulatory networks associated with these genes were comprehensively explored. Our results suggest the causal relationship of PTGS1 and PPBP with IDD secondary to spinal metastases.

PTGS1, also known as cyclooxygenase 1 (COX1), is ubiquitously expressed in various tissues and participates in the biosynthesis of prostaglandin (PG), thereby regulating renal, gastrointestinal, and platelet function [30]. Previous studies have demonstrated that COX1 knockdown can induce caspase-dependent apoptosis, characterized by increased cytosolic cytochrome c levels, caspase-9 and caspase-3 activation, along with downregulation of mitochondria cytochrome c, indicating cytochrome c release from mitochondria into the cytosol [31]. Another study reported that COX-1 could induce mitochondrial apoptosis by mediating Bcl-2 family members in colorectal cancer cells [32]. In addition, PTGS1 has been implicated in mitochondrial dysfunction and is considered a molecular link between inflammation and mitochondrial dysfunction [33]. PTGS1 has been associated with multiple pathological conditions, including inflammation, arthritis, and cancer. Nagao et al. performed a meta-analysis, revealing the association between PTGS variants and nonsteroidal anti-inflamma-

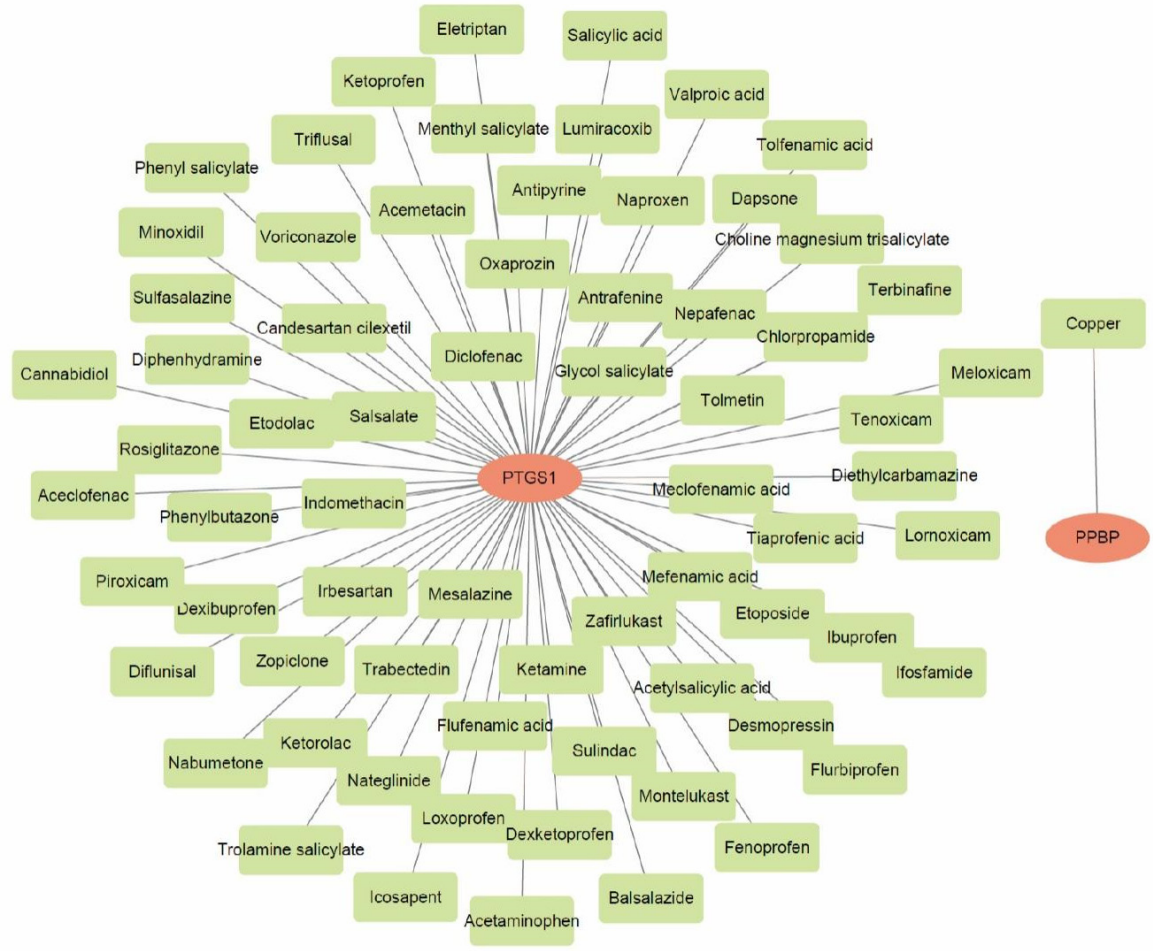

Figure 9. Prediction of biomarker-related drugs.

tory drugs (NSAIDs), which inhibit the biosynthesis of PG by PTGS1 and reduce inflammation [34]. Another study identified PTGS1 as a key candidate gene in inflammatory arthritis based on differential expression in a heterogeneous mouse cohort [35]. Additionally, PTGS1 knockdown was shown to modulate the inflammatory microenvironment during bone remodeling [36]. Elevated PTGS1 expression could impair the protective effects of BCL-2 [37], which may disrupt cellular homeostasis in the nucleus pulposus and contribute to the development of IDD. Moreover, increased PTGS1 expression may reduce the ant-inflammatory effects of BCL-2 by disrupting ECM metabolic balance and enhancing local inflammatory responses in disc cells, thereby promoting IDD progression [38]. Consistent with these findings, the MR analysis in this study supports a potential causal correlation between PTGS1 and IDD.

In addition to mitochondrial regulation, our results also indicate that PTGS1 may also participate in immune modulation. Previous studies have shown that IDD is characterized by infiltration of immune cells, including CD4+ and CD8+ T cells and neutrophils [39]. In this study, PTGS1 was strongly positively correlated with immune cell infiltration, particularly CD4+ cells. This association was subsequently confirmed by the mRNA-TF and ceRNA regulatory network analyses. In addition, subsequent biomarker-drug analysis identified 69 drugs targeting PTGS1. Thus, inhibiting PTGS1 expression may provide clinical benefits for IDD, and in-depth studies into targeted regulation of PTGS1 are warranted.

Pro-platelet basic protein (PPBP), or chemokine (C-X-C motif) ligand 7 (CXCL7), is a small cytokine predominantly expressed in megakaryocytes and produced by monocytes, macro-

phages and endothelial cells, particularly under inflammatory conditions [40]. Moreover, PPBP has also been identified as a biomarker in various diseases, including cancers, thyroid carcinoma, inflammation, and arthritis. Previous research has shown that PPBP modulates immune responses and plays a role in neutrophil-driven inflammation across various pathological conditions [41]. Genetic deletion of PPBP could attenuate skin inflammation and reduce proinflammatory cytokine expression [42]. To date, the association of PPBP with disc degeneration has not been reported. In this study, PPBP was found to be highly expressed during IDD progression. Moreover, PPBP overexpression was positively correlated with the infiltration of CD4+ T cells, mast cells, and memory B cells. Integrating our results with existing literature, we speculated that PPBP may contribute to the formation of a special type of immune microenvironment during the process of IDD by recruiting immune cells, which in turn exacerbates IDD.

Immune infiltration analysis identified seven immune cell types with obvious differences between the IDD and control groups, including activated CD4+ T cells, activated dendritic cells, CD56 dim natural killer cells, mast cell, MDSCs, memory B cells, and regulatory T cells. Among these, PPBP showed the strongest negative associated with activated CD4+ T cells (Cor = 0.75), indicating that PPBP may inhibit the infiltration of activated CD4+ T cell into degenerative disc tissues, thereby suppressing the released of pro-inflammatory cytokines such as IL-6 and TNF-α [43]. In combination with its known roles in maintaining mitochondrial homeostasis and suppressing ferroptosis in NP cells [44], PPBP may collectively attenuate local inflammatory responses and exert anti-inflammatory effects during IDD progression. In contrast, PTGS1 showed an obvious positive association with differential immune cells, particularly mast cells, MDSCs, regulatory T cells, and activated dendritic cells, indicating that PTGS1 may aggravate disc degeneration by promoting the recruitment of pro-inflammatory immune cells and activating NF-κB signaling pathways [45]. The infiltration of these immune cells may further enhance ECM degradation and disrupt the immune-inflammatory microenvironment. Taken together, elevated PPBP expression appears to suppress activated CD4+ T cell infiltration and reduce the inflammation, whereas increased PTGS1 expression promotes immune cells infiltration and aggravates disc degeneration, suggesting the existence of a “balancing regulatory axis” between PPBP and PTGS1 in the inflammatory microenvironment of IDD. Dysregulation of this axis may drive the transition from homeostatic maintenance toward sustained inflammation and degenerative progression.

Drug prediction analysis identified 69 potential drugs targeting PTGS1 (e.g., indomethacin) and one drug targeting PPBP (Copper). Previous studies have demonstrated that abnormal PTGS1 expression can cause mitochondrial dysfunction in disc cells and enhance the release of inflammatory cytokines, including IL-1 [46, 47]. Indomethacin may exert protective effects through binding PTGS1, thereby improving mitochondrial function within the intervertebral disc and attenuating inflammatory signaling pathways. In addition, as a NSAID, indomethacin may also modulate systemic immune responses, given that NSAIDs have been reported to regulate peripheral immune cells [48], which could further influence the local immune microenvironment of the disc [49]. Copper, an essential micronutrient, has been reported to suppress NF-κB-induced inflammation through activating antioxidant signaling pathways [50, 51], which provides a novel treatment perspective for the management of IDD.

This research also has some limitations. First, the analyses were conducted exclusively at the bioinformatic level, without further validation in cell or animal experiments. The findings of this study should be validated in future research, such as through gene knockout animal models or drug repositioning-oriented clinical trials. Second, the data in this study were derived from public databases, including the application of GWAS dataset (e.g., ukb-b-19807) to spinal metastasis- related IDD, and the sample size was small, which may introduce potential bias. Third, the precise mechanisms by which PTGS1 and PPBP promote inflammasome activation remain to be investigated. Fourth, this study focused primarily on RNA-level analyses, and protein-level validation in clinical samples (such as surgically resected intervertebral disc tissue) is warranted.

Conclusion

Immune cells infiltration participates in the pathological process of IDD. By integrating MR analysis, single-gene GSEA analysis, mRNA-TFs network construction and biomarker-drug interaction analysis, PTGS1 and PPBP were identified as signature genes, exhibiting promising diagnostic value and may serve as potential molecular targets for the therapy of IDD.

Acknowledgements

This study was supported by the Key Research and Development Program of Shandong Province (2022CXGC020510).

Disclosure of conflict of interest

None.

Address correspondence to: Rui Xu, Academy of Medical Engineering and Translational Medicine, Tianjin University, No. 92, Weijin Road, Tianjin 300072, China. Tel: +86-022-83612122; Fax: +86-022-83612122; E-mail: xrblue@tju.edu.cn

References

[1] Aebi M. Spinal metastasis in the elderly. Eur Spine J 2003; 12 Suppl 2: S202-213.
[2] Cardia A, Cannizzaro D, Stefini R, Chibbaro S, Ganau M and Zaed I. The efficacy of laser interstitial thermal therapy in the management of spinal metastases: a systematic review of the literature. Neurol Sci 2023; 44: 519-528.
[3] Sawada R, Shinoda Y, Ohki T, Ishibashi Y, Kobayashi H, Matsubayashi Y, Tanaka S and Haga N. End-of-life walking ability in cancer patients with spinal metastases. Jpn J Clin Oncol 2024; 54: 81-88.
[4] Noureldine MHA, Shimony N and Jallo GI. Malignant spinal tumors. Adv Exp Med Biol 2023; 1405: 565-581.
[5] Xia Q, Zhao Y, Dong H, Mao Q, Zhu L, Xia J, Weng Z, Liao W, Hu Z, Yi J, Feng S, Jiang Y and Xin Z. Progress in the study of molecular mechanisms of intervertebral disc degeneration. Biomed Pharmacother 2024; 174: 116593.
[6] Cavazzoni G, Pasini M, Le Maitre CL, Dall'Ara E and Palanca M. Degeneration of the nucleus pulposus affects the internal volumetric strains and failure location of adjacent human metastatic vertebral bodies. Acta Biomater 2025; 194: 258-269.
[7] Resnick D and Niwayama G. Intervertebral disc abnormalities associated with vertebral metastasis: observations in patients and cadavers with prostatic cancer. Invest Radiol 1978; 13: 182-190.
[8] Jonsson B, Petren-Mallmin M, Jonsson H Jr, Andreasson I and Rauschning W. Pathoanatomical and radiographic findings in spinal breast cancer metastases. J Spinal Disord 1995; 8: 26-38.
[9] Sun H, Guo J, Xiong Z, Zhuang Y, Ning X and Liu M. Targeting nucleus pulposus cell death in the treatment of intervertebral disc degeneration. JOR Spine 2024; 7: e70011.
[10] Giorgi C, Marchi S, Simoes ICM, Ren Z, Morciano G, Perrone M, Patalas-Krawczyk P, Borchard S, Jedrak P, Pierzynowska K, Szymanski J, Wang DQ, Portincasa P, Wegrzyn G, Zischka H, Dobrzyn P, Bonora M, Duszynski J, Rimessi A, Karkucinska-Wieckowska A, Dobrzyn A, Szabadkai G, Zavan B, Oliveira PJ, Sardao VA, Pinton P and Wieckowski MR. Mitochondria and reactive oxygen species in aging and age-related diseases. Int Rev Cell Mol Biol 2018; 340: 209-344.
[11] Song C, Xu Y, Peng Q, Chen R, Zhou D, Cheng K, Cai W, Liu T, Huang C, Fu Z, Wei C and Liu Z. Mitochondrial dysfunction: a new molecular mechanism of intervertebral disc degeneration. Inflamm Res 2023; 72: 2249-2260.
[12] Chen Q, Qian Q, Xu H, Zhou H, Chen L, Shao N, Zhang K, Chen T, Tian H, Zhang Z, Jones M, Kwan KYH, Sewell M, Shen S, Wang X, Khan MA, Makvandi P, Jin S, Zhou Y and Wu A. Mitochondrial-targeted metal-phenolic nanoparticles to attenuate intervertebral disc degeneration: alleviating oxidative stress and mitochondrial dysfunction. ACS Nano 2024; 18: 8885-8905.
[13] Song Y, Lu S, Geng W, Feng X, Luo R, Li G and Yang C. Mitochondrial quality control in intervertebral disc degeneration. Exp Mol Med 2021; 53: 1124-1133.
[14] Guo W, Mu K, Li WS, Gao SX, Wang LF, Li XM and Zhao JY. Identification of mitochondria-related key gene and association with immune cells infiltration in intervertebral disc degeneration. Front Genet 2023; 14: 1135767.
[15] Wang Y, Wang Z, Sun J and Qian Y. Identification of HCC subtypes with different prognosis and metabolic patterns based on mitophagy. Front Cell Dev Biol 2021; 9: 799507.
[16] Ritchie ME, Phipson B, Wu D, Hu Y, Law CW, Shi W and Smyth GK. Limma powers differential expression analyses for RNA-sequencing and microarray studies. Nucleic Acids Res 2015; 43: e47.
[17] Ito K and Murphy D. Application of ggplot2 to pharmacometric graphics. CPT Pharmacometrics Syst Pharmacol 2013; 2: e79.
[18] Wang H, Zhao Y, Zhang C, Li M, Jiang C and Li Y. Rab27a was identified as a prognostic bio-

maker by mRNA profiling, correlated with malignant progression and subtype preference in gliomas. PLoS One 2014; 9: e89782.
[19] Langfelder P and Horvath S. WGCNA: an R package for weighted correlation network analysis. BMC Bioinformatics 2008; 9: 559.
[20] Conway JR, Lex A and Gehlenborg N. UpSetR: an R package for the visualization of intersecting sets and their properties. Bioinformatics 2017; 33: 2938-2940.
[21] Wu T, Hu E, Xu S, Chen M, Guo P, Dai Z, Feng T, Zhou L, Tang W, Zhan L, Fu X, Liu S, Bo X and Yu G. clusterProfiler 4.0: a universal enrichment tool for interpreting omics data. Innovation (Camb) 2021; 2: 100141.
[22] Hemani G, Zheng J, Elsworth B, Wade KH, Haberland V, Baird D, Laurin C, Burgess S, Bowden J, Langdon R, Tan VY, Yarmolinsky J, Shihab HA, Timpson NJ, Evans DM, Relton C, Martin RM, Davey Smith G, Gaunt TR and Haycock PC. The MR-base platform supports systematic causal inference across the human phenome. Elife 2018; 7: e34408.
[23] Bowden J, Davey Smith G and Burgess S. Mendelian randomization with invalid instruments: effect estimation and bias detection through egger regression. Int J Epidemiol 2015; 44: 512-525.
[24] Bowden J, Davey Smith G, Haycock PC and Burgess S. Consistent estimation in Mendelian randomization with some invalid instruments using a weighted Median estimator. Genet Epidemiol 2016; 40: 304-314.
[25] Hartwig FP, Davey Smith G and Bowden J. Robust inference in summary data Mendelian randomization via the zero modal pleiotropy assumption. Int J Epidemiol 2017; 46: 1985-1998.
[26] Burgess S, Scott RA, Timpson NJ, Davey Smith G, Thompson SG and Consortium EI. Using published data in Mendelian randomization: a blueprint for efficient identification of causal risk factors. Eur J Epidemiol 2015; 30: 543-552.
[27] Hanzelmann S, Castelo R and Guinney J. GSVA: gene set variation analysis for microarray and RNA-seq data. BMC Bioinformatics 2013; 14: 7.
[28] Su G, Morris JH, Demchak B and Bader GD. Biological network exploration with cytoscape 3. Curr Protoc Bioinformatics 2014; 47: 8.13.1-24.
[29] Perruchoud C, Dupoiron D, Papi B, Calabrese A and Brogan SE. Management of cancer-related pain with intrathecal drug delivery: a systematic review and meta-analysis of clinical studies. Neuromodulation 2023; 26: 1142-1152.
[30] Fitzpatrick FA. Cyclooxygenase enzymes: regulation and function. Curr Pharm Des 2004; 10: 577-588.
[31] Pentland AP, Scott G, VanBuskirk J, Tanck C, LaRossa G and Brouxhon S. Cyclooxygenase-1 deletion enhances apoptosis but does not protect against ultraviolet light-induced tumors. Cancer Res 2004; 64: 5587-5591.
[32] Ding L, Gu H, Lan Z, Lei Q, Wang W, Ruan J, Yu M, Lin J and Cui Q. Downregulation of cyclooxygenase-1 stimulates mitochondrial apoptosis through the NF-kappaB signaling pathway in colorectal cancer cells. Oncol Rep 2019; 41: 559-569.
[33] Wu B, Zeng L, Lin Y, Wen Z, Chen G, Iwakiri R and Fujimoto K. Downregulation of cyclooxygenase-1 is involved in gastric mucosal apoptosis via death signaling in portal hypertensive rats. Cell Res 2009; 19: 1269-1278.
[34] Zhu L, Chen J, Liu Y, Chen W, Liu X and Yang F. Modulation of prostaglandin-endoperoxide synthase 1 by caulis sinomenii: a novel approach to alleviating diabetic peripheral neuropathy through apoptosis inhibition and anti-inflammatory effects. ACS Chem Neurosci 2025; 16: 2435-2449.
[35] Johnsen AK, Valdar W, Golden L, Ortiz-Lopez A, Hitzemann R, Flint J, Mathis D and Benoist C. Genome-wide and species-wide dissection of the genetics of arthritis severity in heterogeneous stock mice. Arthritis Rheum 2011; 63: 2630-2640.
[36] Wang Y, Liu Y, Zhang M, Lv L, Zhang X, Zhang P and Zhou Y. Inhibition of PTGS1 promotes osteogenic differentiation of adipose-derived stem cells by suppressing NF-kB signaling. Stem Cell Res Ther 2019; 10: 57.
[37] Fang Y, Liu X and Su J. Network pharmacology analysis of traditional Chinese Medicine formula Shuang Di Shou Zhen tablets treating nonexudative age-related macular degeneration. Evid Based Complement Alternat Med 2021; 2021: 6657521.
[38] Konturek PC, Konturek SJ, Pierzchalski P, Bielanski W, Duda A, Marlicz K, Starzynska T and Hahn EG. Cancerogenesis in helicobacter pylori infected stomach-role of growth factors, apoptosis and cyclooxygenases. Med Sci Monit 2001; 7: 1092-1107.
[39] Zhang Y, Zhang J, Sun Z, Wang H, Ning R, Xu L, Zhao Y, Yang K, Xi X and Tian J. MAPK8 and CAPN1 as potential biomarkers of intervertebral disc degeneration overlapping immune infiltration, autophagy, and ceRNA. Front Immunol 2023; 14: 1188774.
[40] Wang Y and Ward NL. PPBP/CXCL7: a novel chemokine linking psoriasis to atherosclerosis through endothelial mitochondrial dysfunction. J Invest Dermatol 2025; [Epub ahead of print].
[41] Chen Y, Zhao A, Yang H, Yang X, Cheng T, Rao X and Li Z. Role of fatty acid metabolism-related

genes in periodontitis based on machine learning and bioinformatics analysis. Hua Xi Kou Qiang Yi Xue Za Zhi 2024; 42: 735-747.
[42] Zhu L, Du L, Wu J, Ding D, Wang J, Wang R, Liu Z, Kuzmina N, Wang H, Yang Y, Stahle M, Landen NX, Li S and Li D. Adipose tissue macrophage-derived PPBP exacerbates psoriasis-associated atherosclerosis by inducing mitochondrial dysfunction in aortic endothelial cells. J Invest Dermatol 2025; [Epub ahead of print].
[43] Zhang P, He J, Gan Y, Shang Q, Chen H, Zhao W, Cui J, Shen G, Li Y, Jiang X, Zhu G and Ren H. Unravelling diagnostic clusters and immune landscapes of cuproptosis patterns in intervertebral disc degeneration through dry and wet experiments. Aging (Albany NY) 2023; 15: 15599-15623.
[44] Li W, Zhang S, Zhao Y, Wang D, Shi Q, Ding Z, Wang Y, Gao B and Yan M. Revealing the key MSCs niches and pathogenic genes in influencing CEP homeostasis: a conjoint analysis of single-cell and WGCNA. Front Immunol 2022; 13: 933721.
[45] Wang N, Mi Z, Chen S, Fang X, Xi Z, Xu W and Xie L. Analysis of global research hotspots and trends in immune cells in intervertebral disc degeneration: a bibliometric study. Hum Vaccin Immunother 2023; 19: 2274220.
[46] Song C, Wu X, Chen C, Shen B, Mei Y, Yan Q, Jiang F, Chen F and Liu F. Single-cell analysis integrated with machine learning elucidates the mechanisms of nucleus pulposus cells apoptosis in intervertebral disc degeneration and therapeutic interventions. JOR Spine 2025; 8: e70036.
[47] Blanco FJ, Guitian R, Moreno J, de Toro FJ and Galdo F. Effect of antiinflammatory drugs on COX-1 and COX-2 activity in human articular chondrocytes. J Rheumatol 1999; 26: 1366-1373.
[48] Bosch DJ, Nieuwenhuijs-Moeke GJ, van Meurs M, Abdulahad WH and Struys M. Immune modulatory effects of nonsteroidal anti-inflammatory drugs in the perioperative period and their consequence on postoperative outcome. Anesthesiology 2022; 136: 843-860.
[49] Vaudreuil N, Kadow T, Yurube T, Hartman R, Ngo K, Dong Q, Pohl P, Coelho JP, Kang J, Vo N and Sowa G. NSAID use in intervertebral disc degeneration: what are the effects on matrix homeostasis in vivo? Spine J 2017; 17: 1163-1170.
[50] Persichini T, Percario Z, Mazzon E, Colasanti M, Cuzzocrea S and Musci G. Copper activates the NF-kappaB pathway in vivo. Antioxid Redox Signal 2006; 8: 1897-1904.
[51] Yang D, Xiao P, Qiu B, Yu HF and Teng CB. Copper chaperone antioxidant 1: multiple roles and a potential therapeutic target. J Mol Med (Berl) 2023; 101: 527-542.

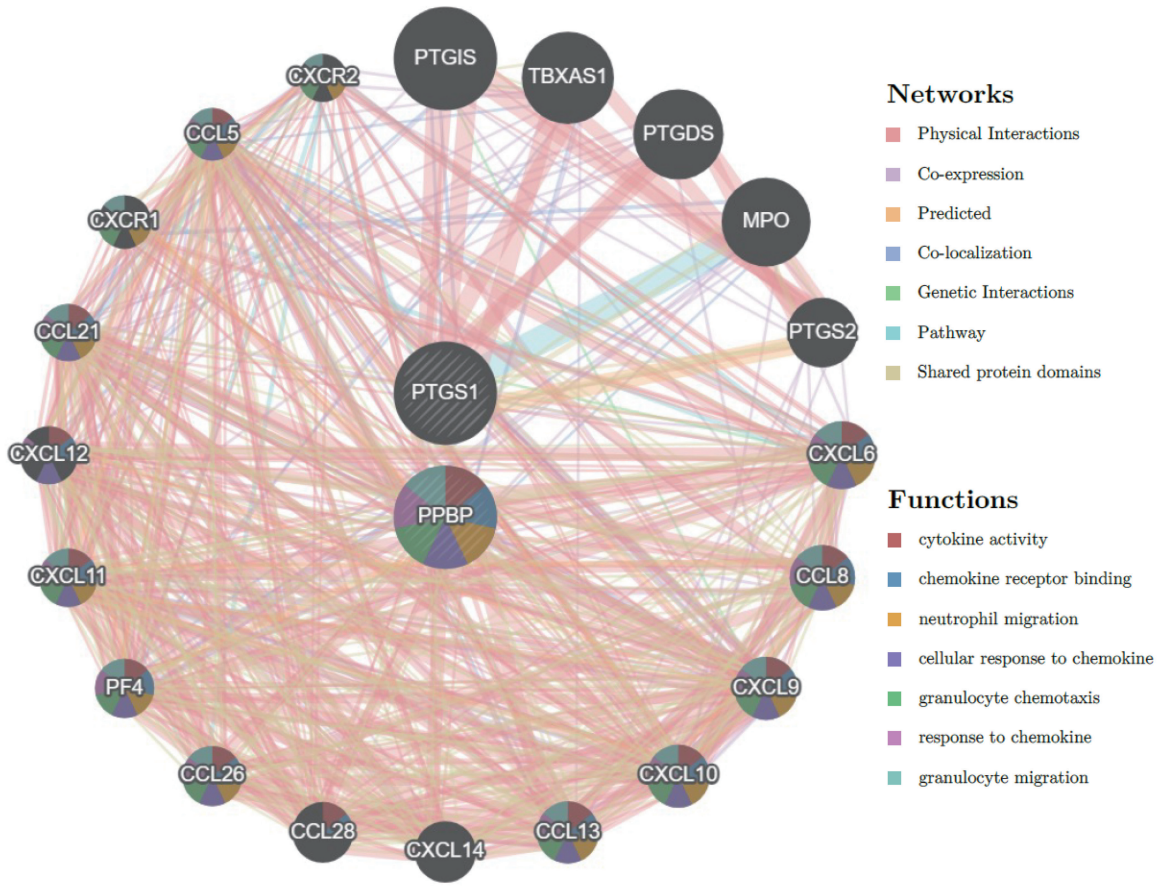

Supplementary Figure 1. The gene-gene interaction network of PTGSI and PPBP.

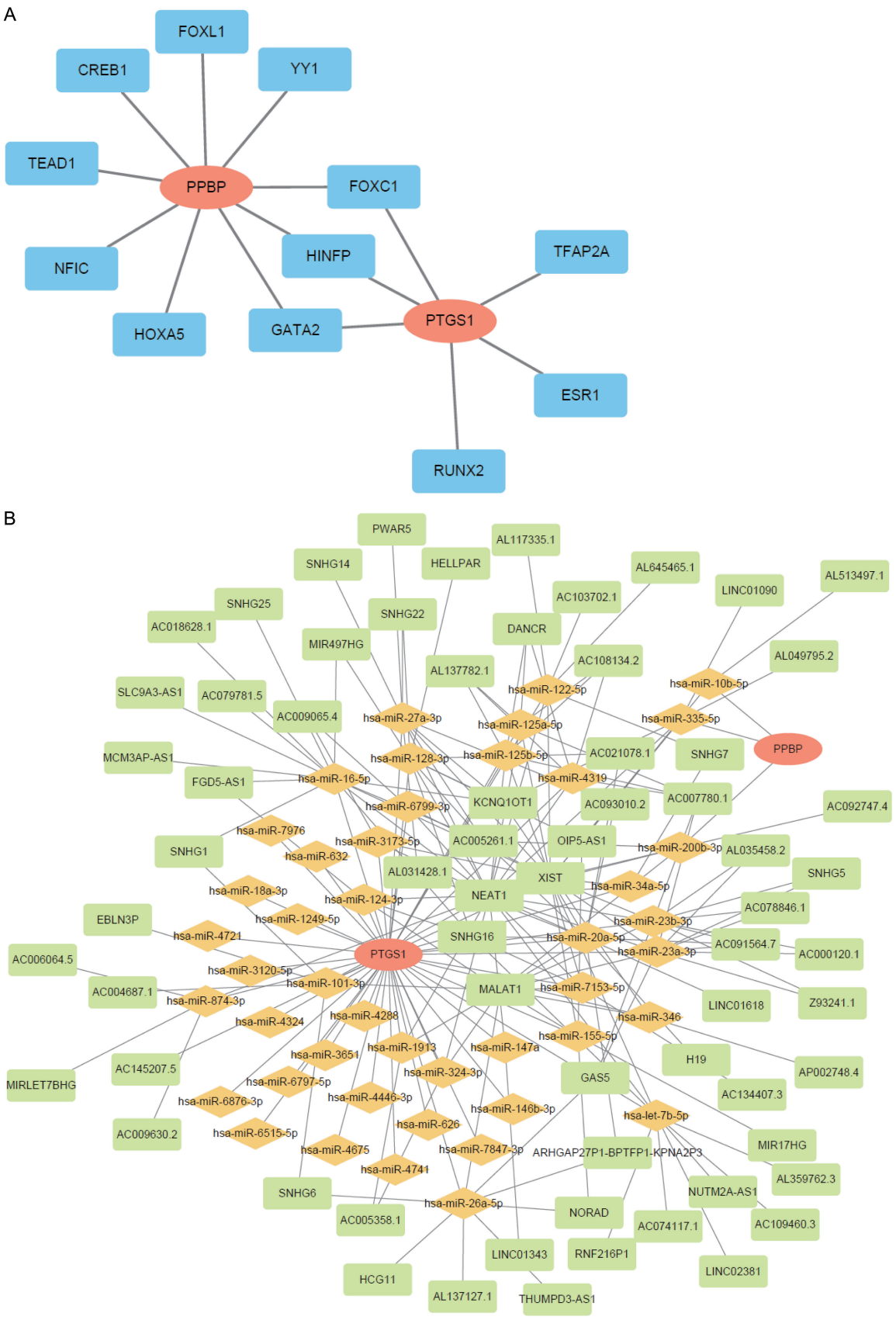

Supplementary Figure 2. The mRNA-TF and ceRNA regulatory networks of biomarkers. A: The mRNA-TF regulatory network. B: The lncRNA-miRNA-mRNA network.